PREPARATION AND PROPERTIES OF RARE-EARTH COMPOUNDS

Semiannual Technical Report
(4 June 1971 to 3 January 1972)

January 4, 1972

by

V. E. Wood, K. C. Brog, A. E. Austin, J. F. Miller
W. H. Jones, Jr., E. W. Collings, and R. D. Baxter

Sponsored By

ADVANCED RESEARCH PROJECTS AGENCY

Under

ARPA Order No. 1588
PRON: W2-71-UX316-D1-DZ
Contract No. DAAH01-70-C-1076

BATTELLE
Columbus Laboratories
505 King Avenue
Columbus, Ohio 43201

Distribution of this Document is Unlimited

UNCLASSIFIED

Security Classification

DOCUMENT CONTROL DATA - R & D

(Security classification of title, body of abstract and indexing annotation must be entered when the overall report is classified)

1 ORIGINATING ACTIVITY (Corporate author)	2a. REPORT SECURITY CLASSIFICATION
Battelle, Columbus Laboratories 505 King Avenue Columbus, Ohio 43201	UNCLASSIFIED 2b. GROUP

3 REPORT TITLE

PREPARATION AND PROPERTIES OF RARE-EARTH COMPOUNDS

4. DESCRIPTIVE NOTES (Type of report and inclusive dates)

Semi-Annual Technical Report (4 June 1971 to 3 January 1972)

5. AUTHOR(S) (First name, middle initial, last name)

Van E. Wood, Kenneth C. Brog, Alfred E. Austin, James F. Miller, William H. Jones, Jr., Edward W. Collings, and Ronald D. Baxter

6. REPORT DATE	7a. TOTAL NO OF PAGES	7b. NO. OF REFS
January 4, 1972	39	26

8a. CONTRACT OR GRANT NO	9a. ORIGINATOR'S REPORT NUMBER(S)
DAAH01-70-C-1076 b. PROJECT NO	Battelle Project G-0550
c. d.	9b. OTHER REPORT NO(S) (Any other numbers that may be assigned this report)

10. DISTRIBUTION STATEMENT

Distribution of this document is unlimited.

11 SUPPLEMENTARY NOTES	12. SPONSORING MILITARY ACTIVITY
	Advanced Research Projects Agency Arlington, Virginia 22209

13 ABSTRACT

Preparation, characterization, and physical properties of rare-earth compounds of technological potential are described. Work was in the areas of magnetoferroelectric materials and of narrow-band narrow-gap semiconductors. In the former area, the primary objective is to develop a simultaneously ferroelectric and ferromagnetic device element operating in a useful temperature range. Solid solutions of rare-earth manganites, chromites, and ferrites have been the main object of investigation. Among the presumably ferroelectric hexagonal-form solid solutions studied only $YbMn_{.95}Cr_{.05}O_3$ was determined to be weakly ferromagnetic, and this only below 50 K. Most of the orthorhombic-form materials studied are weakly ferromagnetic; determination of whether any of them is ferroelectric or possesses the prerequisite for ferroelectricity of a polar axis appears to require the preparation of crystalline samples of fairly low conductivity; work on this is progressing. Narrow-band narrow-gap semiconductors undergoing purely electronic semiconductor-to-metal transitions are of considerable practical and fundamental interest. The transitions investigated during the past six months were the pressure-induced ones in the Sm chalcogenides. It was found that a discontinuous transition at 18 kbar in polycrystalline $SmS_{.75}Se_{.25}$ was related to breakup of a minor Sm-rich interfacial phase. Work is continuing on solid solutions of similar composition. Some of these materials display strong white cathodoluminescence.

DD FORM 1 NOV 68 1473

UNCLASSIFIED

Security Classification

UNCLASSIFIED
Security Classification

14 KEY WORDS	LINK A		LINK B		LINK C	
	ROLE	WT	ROLE	WT	ROLE	WT
Magnetoferroelectric Materials						
Semiconducting Compounds						
Semiconductor-to-metal transitions						
Rare-earth manganites						
Rare-earth chromites						
Rare-earth ferrites						
Rare-earth chalcogenides						
Cathodoluminescence						

UNCLASSIFIED
Security Classification

PREPARATION AND PROPERTIES OF RARE-EARTH COMPOUNDS

Semiannual Technical Report
(4 June 1971 to 3 January 1972)

January 4, 1972

by

V. E. Wood, K. C. Brog, A. E. Austin, J. F. Miller
W. H. Jones, Jr., E. W. Collings, and R. D. Baxter

Sponsored By

ADVANCED RESEARCH PROJECTS AGENCY

Under

ARPA Order No. 1588
PPON: W2-71-UX316-D1-DZ
Contract No. DAAH01-70-C-1076

Project Technical Director: V. E. Wood
Phone Number: (614) 299-3151, Ext. 2780

Effective Date: 4 June 1971
Expiration Date: 3 June 1972
Contract Amount: $199,000
Monitored by U.S. Army Missile Command

BATTELLE
Columbus Laboratories
505 King Avenue
Columbus, Ohio 43201

SUMMARY

Preparation, characterization, and physical properties of rare-earth compounds of technological potential are described. Work was in the areas of magnetoferroelectric materials and of narrow-band narrow-gap semiconductors. In the former area, the primary objective is to develop a simultaneously ferroelectric and ferromagnetic device element operating in a useful temperature range. Solid solutions of rare-earth manganites, chromites, and ferrites have been the main object of investigation. Among the presumably ferroelectric hexagonal-form solid solutions studied only $YbMn_{.95}Cr_{.05}O_3$ was determined to be weakly ferromagnetic, and this only below 50 K. Most of the orthorhombic-form materials studied are weakly ferromagnetic; determination of whether any of them is ferroelectric or possesses the prerequisite for ferroelectricity of a polar axis appears to require the preparation of crystalline samples of fairly low conductivity; work on this is progressing. Narrow-band narrow-gap semiconductors undergoing purely electronic semiconductor-to-metal transitions are of considerable practical and fundamental interest. The transitions investigated during the past six months were the pressure-induced ones in the Sm chalcogenides. It was found that a discontinuous transition at 18 kbar in polycrystalline $SmS_{.75}Se_{.25}$ was related to breakup of a minor Sm-rich interfacial phase. Work is continuing on solid solutions of similar composition. Some of these materials display strong white cathodoluminescence.

TABLE OF CONTENTS

LIST OF TABLES

LIST OF FIGURES

INTRODUCTION

The general objective of this program is the development of the device potential of some rare-earth compounds using hitherto unexploited physical properties. These properties (ferromagnetoferroelectricity and semiconductor-metal transitions) have not been made use of principally because of the lack of materials exhibiting them in sufficient degree at reasonable temperatures; consequently, our program thus far has largely concentrated on developing such materials. Further background concerning these phenomena and an account of our previous work are to be found in the Annual Report (AD 726 201) on this project, issued 30 June, 1971. The two principal areas of study in the past 6 months, magnetoelectric materials and narrow-band narrow-gap semiconductors, will be discussed in turn.

MAGNETOELECTRIC MATERIALS

Background

The aim of this work is the development of a material simultaneously displaying ferroelectricity and ferromagnetism in a useful temperature range, preferably at room temperature. Such a material would have a number of unique memory and signal-processing capabilities. There are also potential applications for materials which are ferroelectric and antiferromagnetic, and as well for materials whose effective dielectric polarizability can be altered by an external magnetic field.[1] In the latter case, however,

ferroelectric and ferromagnetic order seems desirable to maximize the magnitude of the effect.[2]

Our recent work has been largely directed toward the following questions:

1) The hexagonal heavy-rare-earth manganites, (RE)MnO_3, are known to be ferroelectric, with high transition temperatures (>900 K), but to be antiferromagnetic below about 90 K (some weakly ferromagnetic below 10 K)[3]. Can weak ferromagnetism at higher temperatures be induced in this structure by alloying with Fe or Cr? (It is presumed for the time being that introduction of moderate amounts of other 3d ions does not destroy the ferroelectricity as long as the hexagonal structure is retained, although the transition temperature might be significantly reduced.)

2) It has been maintained[4] that certain of the weakly ferromagnetic (below 120 K) orthorhombic rare-earth orthochromites, $RECrO_3$, are ferroelectric below about 700-800 K, although this has been disputed.[5] Does ferroelectricity in fact occur in these or related compounds?

3) It is claimed[6] that certain solid solutions between ferroelectric $BiFeO_3$ and weakly ferromagnetic rare-earth orthoferrites, $REFeO_3$, are simultaneously ferroelectric and ferromagnetic near room temperature and below. Can this be verified, and how do the electrical and magnetic properties depend on the rare earth used?

Before describing recent experiments and their interpretation in some detail, we will summarize the current status of our thinking on each of these questions.

1) Although extensive solid solution of Fe into the hexagonal rare-earth manganites was found for the compounds with smaller rare-earth

cations Yb and Lu, all the hexagonal materials produced seem to be antiferromagnetic. Interpretation is complicated by the tendency of small amounts of rare-earth iron garnet to form. In the $YbMn_xCr_{1-x}O_3$ system, there appears to be an intrinsic small magnetic moment in the composition at the limit of solubility in the hexagonal phase, $YbMn_{.95}Cr_{.05}O_3$, but this moment only occurs below 50 K; so this material is probably not superior to other established low-temperature ferromagnetoferroelectrics such as nickel iodine boracite.[7] Interesting properties of the high-pressure orthorhombic modification of $YbFe_{.5}Mn_{.5}O_3$ are discussed below.

2) It has been shown (see Annual Report) that resistivity anomalies are not a satisfactory way of detecting ferroelectric transitions in rare-earth manganites or chromites. Lattice parameter changes cannot be relied on either.[8] A number of other methods for detecting ferroelectricity or just acentricity have been found to be inconclusive owing mainly to the relatively high conductivity of the ceramic-type specimens prepared so far. As discussed below, considerable effort is now being devoted to preparation of crystalline specimens. Even when these are obtained, considerable work on controlling conductivity may be necessary.

3) Preparation of $Bi_{1-x}Nd_xFeO_3$ solid solutions is just getting under way. It is expected that study of these and related materials will form a considerable part of the work of the forthcoming six months.

Preparation and Characterization

In the first two subsections of this section we describe the initial preparation, transformation (if any), and characterization of the ferromanganite and manganite-chromite samples on which the magnetic measurements described in the following section were made. In the last three

subsections, experiments on crystal growth, vapor deposition, and preparation of new materials are discussed.

$HoMn_{1-x}Fe_xO_3$ and $LuMn_{1-x}Fe_xO_3$ Materials

Powder specimens of the $HoMn_{1-x}Fe_xO_3$ and $LuMn_{1-x}Fe_xO_3$ materials were prepared by direct reaction of oxides utilizing general procedures that have been described previously (see Annual Report). In each case, stoichiometric proportions of all constituents were taken into solution. An initimate mixture of the nitrates was prepared by adding a large excess of concentrated nitric acid and evaporating to dryness. The desired compound was obtained by raising the temperature to decompose the nitrates, then reacting the resulting intimate mixture of oxides at elevated temperatures. The $HoMn_{1-x}Fe_xO_3$ materials were reacted as powders for 24 hours at 1175 C in air, then were pressed and reacted in pellet form for 26 hours at 1275 C in oxygen. The $LuMn_{1-x}Fe_xO_3$ materials were reacted as powders for two periods at 1175 C, with interim mixing, then were pressed and reacted in pellet form for 24 hours at 1300 C in oxygen.

The system $HoMnO_3$-$HoFeO_3$ has extensive solid solution of $HoMnO_3$ in orthorhombic $HoFeO_3$ to beyond $HoMn_{.75}Fe_{.25}O_3$. Table 1 gives the phase analysis of compositions prepared in this system. The unit cell parameters of single phase solid solutions are listed in Table 2. Any solid solution of $HoFeO_3$ in hexagonal $HoMnO_3$ is quite limited, probably less than 1.0 molar percent.

The system $LuMnO_3$-$LuFeO_3$ has solid solution of $LuFeO_3$ in hexagonal $LuMnO_3$ up to $LuMn_{.5}Fe_{.5}O_3$. The phases for various compositions are given

in Table 1 while the unit cell parameters of the solid solutions are listed in Table 2. This system is similar to $YbMnO_3$-$YbFeO_3$.

The differences in solubility of Mn^{3+} in rare-earth ferrites from holmium to lutetium appear to be dependent upon the size and oxygen coordination of the rare-earth ion. Thus the ionic radii (for 8-fold coordination) decrease from 1.02Å for Ho^{3+} to 0.97Å for Lu^{3+}. In the rare earth orthoferrites, the RE-O coordination changes with increasing ion radius.[9] For Lu to Er the first eight oxygens may be considered as six nearest neighbors with the RE-O distance increasing with rare earth radius and 2 oxygens at an intermediate distance which actually decreases from Lu to Er and then increases after Ho. The other 4 oxygens are next-nearest neighbors and have decreasing rare-earth-to-oxygen distance with increasing rare-earth radii. This shift in oxygen-ion coordination about the rare-earth ion may limit the accommodation, because of the increased distortion of the oxygen octahedron about Mn^{3+} compared to that for Fe^{3+}.

$YbMn_{1-x}Fe_xO_3$ and $YbMn_{1-x}Cr_xO_3$ Materials

The solid solution $YbMn_{.5}Fe_{.5}O_3$ was transformed from the hexagonal to the orthorhombic phase at 1000 C under 40 kbar. The unit cell parameters are given in Table 2.

The high-pressure phase, termed $YbMnO_3$ III, found in earlier studies on $YbMnO_3$ has been identified as YbOOH. This phase was made by reaction of $YbMnO_3$ with H_2O in sealed platinum capsules. The presence of adsorbed water causes partial decomposition of $YbMnO_3$ at 30 to 40 kbar and 900-1100 C. Drying of the powdered material before sealing eliminates this decomposition. Adsorbed water does not affect the stability of the chromite phase.

TABLE 1

PHASE ANALYSIS OF $HoMnO_3$-$HoFeO_3$ AND $LuMnO_3$-$LuFeO_3$

Composition	Phase (type)
$HoMnO_3$	Hex-$HoMnO_3$
$HoMn_{.75}Fe_{.25}O_3$	Ortho-$HoFeO_3$ solid solution
$HoMn_{.5}Fe_{.5}O_3$	" " " "
$HoMn_{.25}Fe_{.75}O_3$	" " " "
$HoFeO_3$	Ortho-$HoFeO_3$ + Ho_2O_3 + $Ho_3Fe_5O_{12}$
$LuMnO_3$	Hex-$LuMnO_3$
$LuMn_{.75}Fe_{.25}O_3$	Hex-$LuMnO_3$ solid solution + trace Lu_2O_3
$LuMn_{.5}Fe_{.5}O_3$	Hex-$LuMnO_3$ solid solution + trace Lu_2O_3 + trace $Lu_2Fe_5O_{12}$ (by microprobe)
$LuMn_{.6}Fe_{.4}O_3$	Hex-$LuMnO_3$ + Ortho-$LuFeO_3$ + trace Lu_2O_3

TABLE 2

CRYSTAL STRUCTURE DATA ON RARE-EARTH MANGANITES, CHROMITES, AND FERRITES

Compound	Hexagonal			Orthorhombic			
	a_o	c_o	Ω	a_o	b_o	c_o	Ω
$YbMn_{.9}Cr_{.1}O_3$				5.22	5.70	7.33	55.0
$YbMn_{.75}Cr_{.25}O_3$				5.20	5.69	7.38	54.7
$YbMn_{.5}Cr_{.5}O_3$				5.20	5.60	7.42	54.0
$YbMn_{.25}Cr_{.75}O_3$				5.19	5.55	7.46	53.7
$YbMn_{.5}Fe_{.5}O_3$				5.22	5.64	7.44	54.5
$HoMn_{.75}Fe_{.25}O_3$				5.26	5.66	7.47	55.6
$HoMn_{.5}Fe_{.5}O_3$				5.26	5.61	7.53	55.7
$LuMnO_3$	6.04	11.37	59.9				
$LuMn_{.75}Fe_{.25}O_3$	6.04	11.44	60.2				
$LuMn_{.5}Fe_{.5}O_3$	6.00	11.50	59.8				

a_o, b_o, c_o - unit cell parameters in angstroms

Ω - volume per formula unit (A^3)

The orthorhombic solid solutions of compositions $YbCr_{1-x}Mn_xO_3$ ($x = 0.5$, 0.75 and 0.9) were prepared by further reaction at 1000 C and 60 kbar pressure of the two-phase materials of previous reaction at 1300 C in 1 atmosphere of O_2. These together with $YbCr_{.75}Mn_{.25}O_3$ provided a set of samples for determination of the effect of Mn/Cr ratio on the magnetic properties. The orthorhombic unit cell parameters are given in Table 2. Fig. 1 shows the changes from $YbMnO_3$ to $YbCrO_3$ as an increase in c_o, and a decrease in b_o and in unit-cell volume, with little change in a_o.

Chemical Vapor Deposition of $YMnO_3$

The experiments on the growth of $YMnO_3$ by chemical vapor deposition have demonstrated that $YMnO_3$ is produced by oxidation of YCl_3 and $MnCl_2$ vapors at 1000 to 1200 C. The YCl_3 needed to be purified by sublimation under CCl_4 atmosphere to eliminate YbOCl. The YCl_3 and $MnCl_2$ vapors react upon contact with wet oxygen at about 1000 C to yield $YMnO_3$ powder instead of reaction at hotter surfaces, 1100 to 1150 C, to deposit as an adherent film. Since the temperature of the YCl_3 vapor needs to be about 1000 C for adequate vapor transport, the temperature control for film formation appears to be more critical than for ferrites or garnets which require about 1200 C for reaction. The temperature difference for reaction would also make questionable the deposition of solid solutions, such as ferrites with manganites. Therefore, these experiments were stopped. The $YMnO_3$ powder produced is bright blue in color, but otherwise seems similar to that prepared by solid-state reaction.

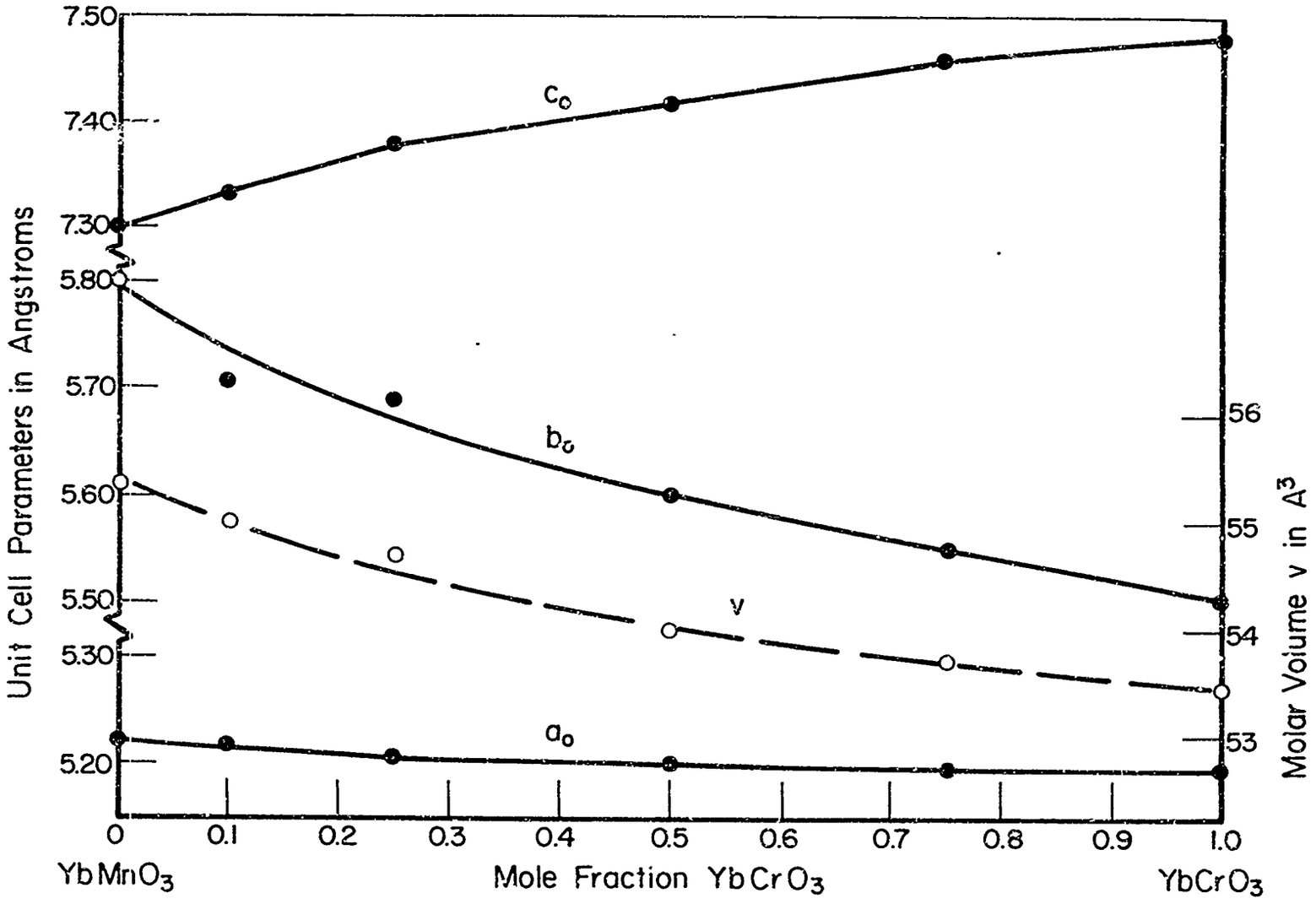

FIGURE 1. Lattice parameters and molar volume of orthorhombic $YbMn_{1-x}Cr_xO_3$ solid solutions.

Flux Growth of $YbCrO_3$ and $YbMnO_3$

The objective of the work on the growth of single crystals is to obtain single crystals of sufficient size for tests of acentricity and ferroelectricity. Lead fluoride-lead oxide fluxes have been used prevalently for the growth of ortho-ferrites and orthochromites. However, since traces of Pb, and also Bi, could greatly complicate interpretation of the tests by affecting the electrical properties of the material and since Pb fluxes have been found unsatisfactory for the manganites,[10] it was decided that fluxes containing Pb or Bi would be avoided, if possible. Thus exploratory work was undertaken utilizing the slow-cool growth method and solvents that have been reported suitable for the growth of ferrites, Cr_2O_3, and chromium spinels, and compounds containing Mn_2O_3. The solvents investigated included $K_2O \cdot xB_2O_3$,[9] $BaO \cdot xB_2O_3$,[11] $xBaO \cdot yBaF_2 \cdot 2B_2O_3$,[12] $Na_2B_4O_7$,[13] and $K_2B_4O_7$[13] that have been employed for the growth of ferrites and Fe_2O_3. It can be said as a general conclusion that solvents from this group appeared unsatisfactory for the growth of $YbCrO_3$ because, in these basic solvents in air, chromium is oxidized to the hexavalent state. As is indicated in the first portion of Table 3, chromates were formed. Borates also were observed to form, and, when Mn was present, alkaline-earth manganite was noted to form, rather than $YbMnO_3$, under the conditions that prevailed.

Exploratory investigation also was made of the growth of $YbCrO_3$ crystals in Bi_2O_3 flux. Although rare-earth orthochromite crystals reportedly have been grown in Bi_2O_3 in platinum containers,[14] our work has been hampered by failure of the platinum crucibles with some failing when the materials were premelted, within a few hours and at temperatures as low as 1070 C. The one slow-cool growth run that was completed, utilizing a 25 mole percent

TABLE 3

SUMMARY OF SOME FLUX GROWTH RUNS

Specimen No.	Compound	Solvent	Maximum Temperature, °C	Phase Identified
28886-10	$YbCrO_3$	KBO_2	1250	K_2CrO_4, minor Yb_2O_3, minor $YbCrO_3$.
-19	$YbCrO_3$	$K_2B_4O_7$	1150	K_2CrO_4, $YbBO_3$.
-22	$YbCrO_3$	KBO_2	1025	$YbBO_3$, $MnBO_3$.
-34	$YbMnO_3$	$0.18BaF_2$-$0.41BaO$-$0.41B_2O_3$	1175	$BaMnO_3$, BaBOF, YbOF, $YbBO_3$.
-38	$YbCrO_3$	"	1250	$BaCrO_4$
-42	$YbMn_{.5}Cr_{.5}O_3$	$Na_2W_2O_7$-Na_2WO_4	1200	Yb Tungstate
-43	"	"	1250	Mn_2O_3, Yb tungstate
-51	"	Bi_2O_3	1225	Small amount hex. $YbMnO_3$ phase + Yb_2O_3

solution of $YbCrO_3$ in Bi_2O_3 and slow cool from 1225 C at 6 C per hour yielded orthorhombic $YbCrO_3$, but no visible crystals.

The polytungstate $xNa_2W_2O_7$-yNa_2WO_4 flux, which has been reported[15] to be a suitable flux for the growth of transition-metal chromium and iron spinels including $MnCr_2O_4$ and $Y_3Fe_5O_{12}$, also has been investigated as a solvent for $YbCrO_3$. In this work, compositions analogous to those used for the chromium spinels were employed, along with maximum temperatures in the range 1200-1275 C and cooling rates of 1.2 and 2.5 C per hour. Although the chromite appears to go into solution, compositions investigated to date have not yielded the $YbCrO_3$ phase.

In future work, it is planned that other composition ranges in the pseudoternary $Na_2W_2O_7$-Na_2WO_4-$YbCrO_3$ system will be explored and that inert atmospheres (with the basic fluxes) will be investigated.

$Bi_xNd_{1-x}FeO_3$ Materials

The investigation of solid solutions between ferroelectric $BiFeO_3$ and weakly ferromagnetic $(RE)FeO_3$ was started with the $Bi_xNd_{1-x}FeO_3$ system.

In the preparation of polycrystalline powder specimens of these materials, the direct reaction of oxides is again being employed. However, in this case the intimate mixture of oxides is being prepared by chemical co-precipitation. Stoichiometric proportions of the constituents are taken into an acid solution. The excess acid then is rapidly neutralized with an excess ammonium hydroxide solution, thus precipitating an intimate mixture of hydroxides. After washing thoroughly, the mixture is fired to dehydrate the material and carry out the solid-state reaction. The final firing temperature is being held at 780 C, below the reported decomposition

temperature of $BiFeO_3$.[16] First preparations of samples in this system have been completed and the materials are being analyzed.

Magnetic Properties

Rather extensive magnetic susceptibility measurements have been carried out on more-or-less homogeneous solid solutions in the $YbMn_{1-x}Fe_xO_3$, $LuMn_{1-x}Fe_xO_3$, and $YbMn_{1-x}Cr_xO_3$ systems. The goals of these measurements are

1) to determine the region of magnetic ordering, if any, in these materials, and

2) to elucidate the nature of the magnetic interactions in these materials, in order to determine how the magnetic properties might be optimized. Susceptibility measurements are also frequently useful for detection of impurity phases.

There have been two difficulties to overcome in making and interpreting these measurements. First, it was found that false effects in the 5-12 K range could occur as a result of eddy-current heating of the sample holder when the magnetic field was cycled to high values. This problem has been greatly alleviated by use of a new, predominantly non-conducting sample holder. Second, because the magnetic moments found are generally quite small, it is frequently difficult to separate the effects due to the bulk of the sample from those of magnetic impurities. There are a number of things one can do about this:

a) Since different samples, even from the same lot, often have different amounts of impurities, repetition of measurements on different samples frequently shows that an observed moment results from an impurity.

Because of uncertainties concerning sample mass, this is not such a good method for impurities magnetic only at low temperatures (< 77 K).

b) A number of impurities arise from slight decomposition (O_2 loss) of these ceramic oxides. This decomposition may be speeded up by cycling the sample to high temperature or by holding it for extended periods at low pressure. Subsequent magnetic measurements then clearly reveal a moment as due to an impurity.

c) When an impurity has been tentatively identified, it is often possible to prepare new samples, under different firing conditions or with slightly altered proportions of starting materials, which contain less (or none) of this particular impurity.

d) If the magnetization of a suspected impurity is known to vary as $(T-T_c)^{1/2}$ near the transition temperature T_c, a plot of M^2 vs T should contain a substantial straight-line region with intercept near T_c. (Other magnetic "signatures" of certain impurities, such as compensation temperatures, might be of use in some cases.)

e) If the high-field susceptibility should show the lambda-like anomaly characteristic of antiferromagnetic ordering, any moment persisting through the transition is presumably due to an impurity, since the majority phase cannot be antiferromagnetic and ferromagnetic at the same time.

f) When enough members of a solid-solution series are studied, systematic trends may emerge, sudden deviations from which may be attributed to impurity effects.

g) Electron microprobe traverses have frequently been used to detect impurity phases at an appropriate level of segregation.

All these fairly obvious techniques have been applied as seemed appropriate, all in all very successfully.

We will describe briefly the results on each of the alloy systems treated.

i) $YbMn_{1-x}Fe_xO_3$ - The limit of homogeneity in the hexagonal phase was found to lie between x = .5 and x = .6. Susceptibility measurements have been made in the temperature range 4.2 to 700 or 800 K on two hexagonal-phase samples of the composition $YbMn_{.5}Fe_{.5}O_3$ (one reprocessed), on one hexagonal-phase sample of $YbMn_{.75}Fe_{.25}O_3$, and on one sample of $YbMn_{.5}Fe_{.5}O_3$ transformed to the orthorhombic form, as well as on both forms of $YbMnO_3$. No conclusive evidence of any intrinsic magnetic moment was found in any of the hexagonal specimens. Samll apparent moments that occurred were attributed, using methods (a), (b) and (c) above, to garnet ($Yb_3Fe_5O_{12}$) impurities at the few tenths of 1 percent level and, in some cases, to even smaller amounts of iron oxides. No antiferromagnetic ordering of the 3d-ions was apparent from the susceptibility measurements, though given the lack of an intrinsic moment, such ordering seems likely in all the hexagonal materials. The presence of minor magnetic phases may make it more difficult to determine the characteristic magnetic parameters of the predominant phase; one extreme case of this is shown among the high-temperature parameters plotted in Fig. 2. Since we have not yet made any susceptibility measurements on the orthorhombic $HoMn_{1-x}Fe_xO_3$ solid solutions, we have also included in Fig. 2 data on some of these reported by Apostolov and Pataud.[17] It is by no means certain that their samples (particularly with x = .3 and .5) were entirely homogeneous, though. Strangely, simple magnetic susceptibility data do not seem ever to have been reported for $YbFeO_3$.

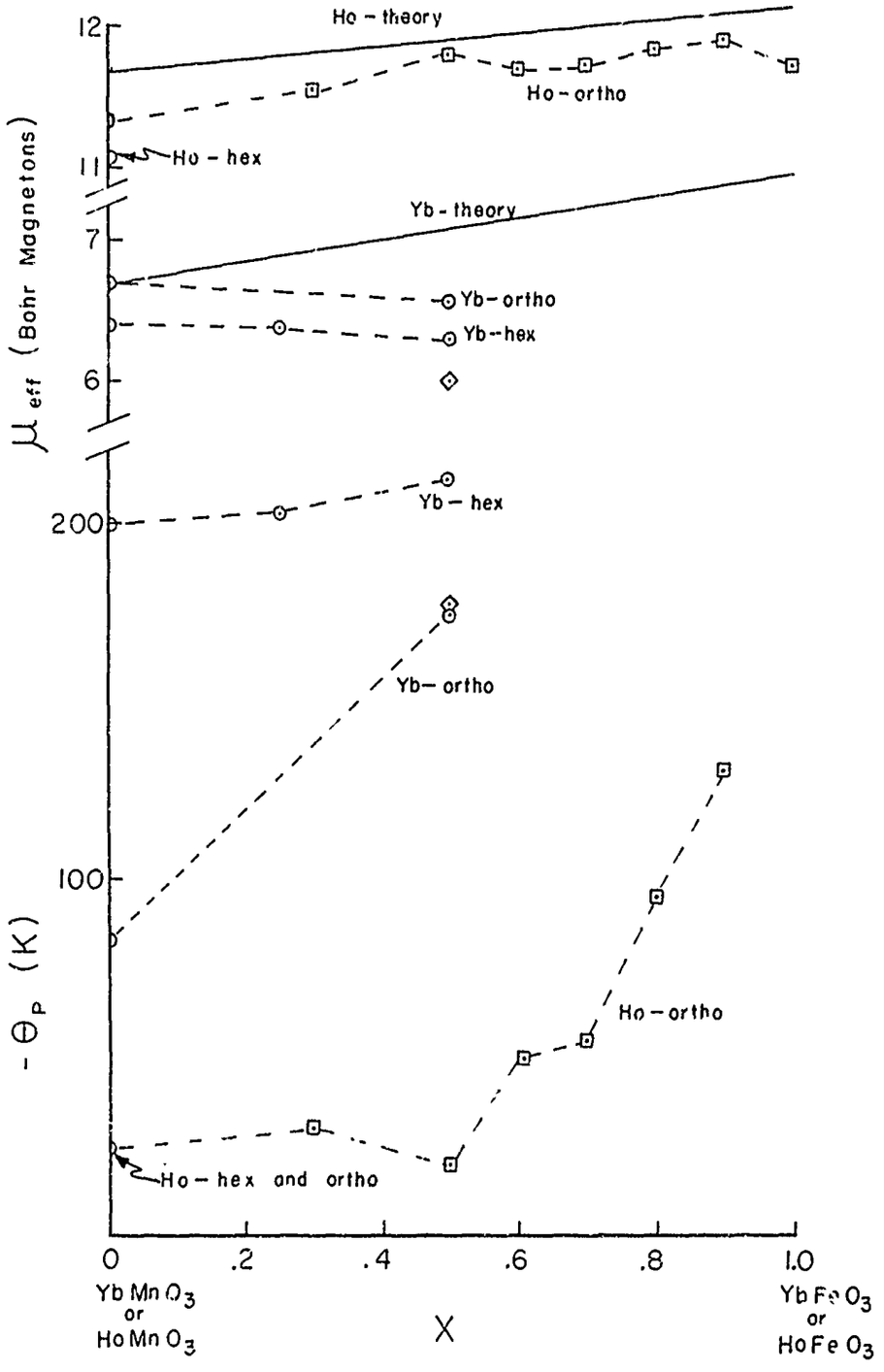

FIGURE 2. High-temperature magnetic properties of $YbMn_{1-x}Fe_xO_3$ and $HoMn_{1-x}Fe_xO_3$ solid solutions. Plotted are the parameters in the equation $\chi = N_o\mu_B{}^2\mu_{eff}{}^2/3k(T-\theta_p)$. Diamonds: data on less pure hex-$YbMn_{.5}Fe_{.5}O_3$ sample. Squares: data of Apostolov and Pataud (Ref. 17).

The orthorhombic modification of $YbMn_{.5}Fe_{.5}O_3$ is weakly ferromagnetic, possessing a moment only between about 180 and 440 K (Fig. 3). The maximum moment developed is about .008 Bohr magnetons/formula unit at about 250 K. This is about an eighth of the room temperature moment in $YbFeO_3$. No significant changes in the high-field susceptibility occur in the range where the moment exists. Low temperature measurements to determine whether a moment reoccurs have not yet been made, but it is clear that there is essentially no moment between 77 and 180 K. It is conceivable that the ordering changes to antiferromagnetic below 180 K. Similar effects were described by Polyakov and co-workers[18] in the $YMn_{1-x-y}Fe_xAl_yO_3$ system. It would seem that by sufficient tinkering one could get some materials of this sort with upper or lower transition temperature, or both, near room temperature. This could enhance the attractiveness of these modified orthoferrites for some applications, particularly for displays and other magnetooptical devices.

ii) $LuMn_{1-x}Fe_xO_3$ - In an attempt to increase the solubility of iron in the hexagonal-form ferromanganites a number of samples were prepared in which Yb was replaced by the yet smaller ion of Lu. The range of solid solubility turned out to be increased little, if at all, by this substitution, though, remaining between x = .5 and .6. The magnetic susceptibilities of hexagonal $LuMnO_3$, $LuMn_{.75}Fe_{.25}O_3$ and $LuMn_{.5}Fe_{.5}O_3$ were measured from 77 to 700 K. No regions of ferromagnetism were found. An apparent moment found in $LuMn_{.5}Fe_{.5}O_3$ was shown by methods (d), (e) and (g) to result from the presence of about 1 percent of garnet, $Lu_3Fe_5O_{12}$. The inverse susceptibilities are shown in Fig. 4. The high-temperature susceptibility for $LuMnO_3$ shows considerable field dependence; thus χ_∞ is

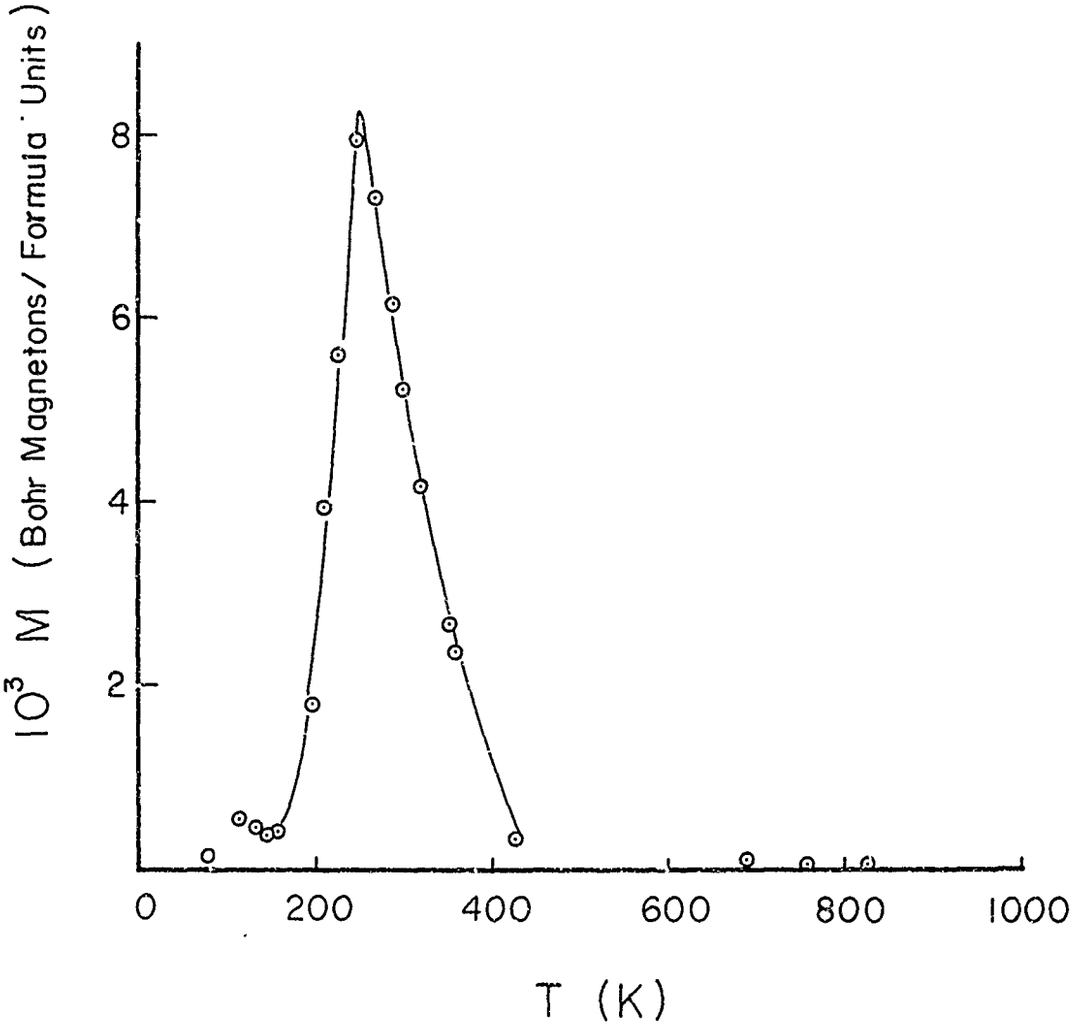

FIGURE 3. Spontaneous magnetic moment of orthorhombic modification of $YbMn_{.5}Fe_{.5}O_3$

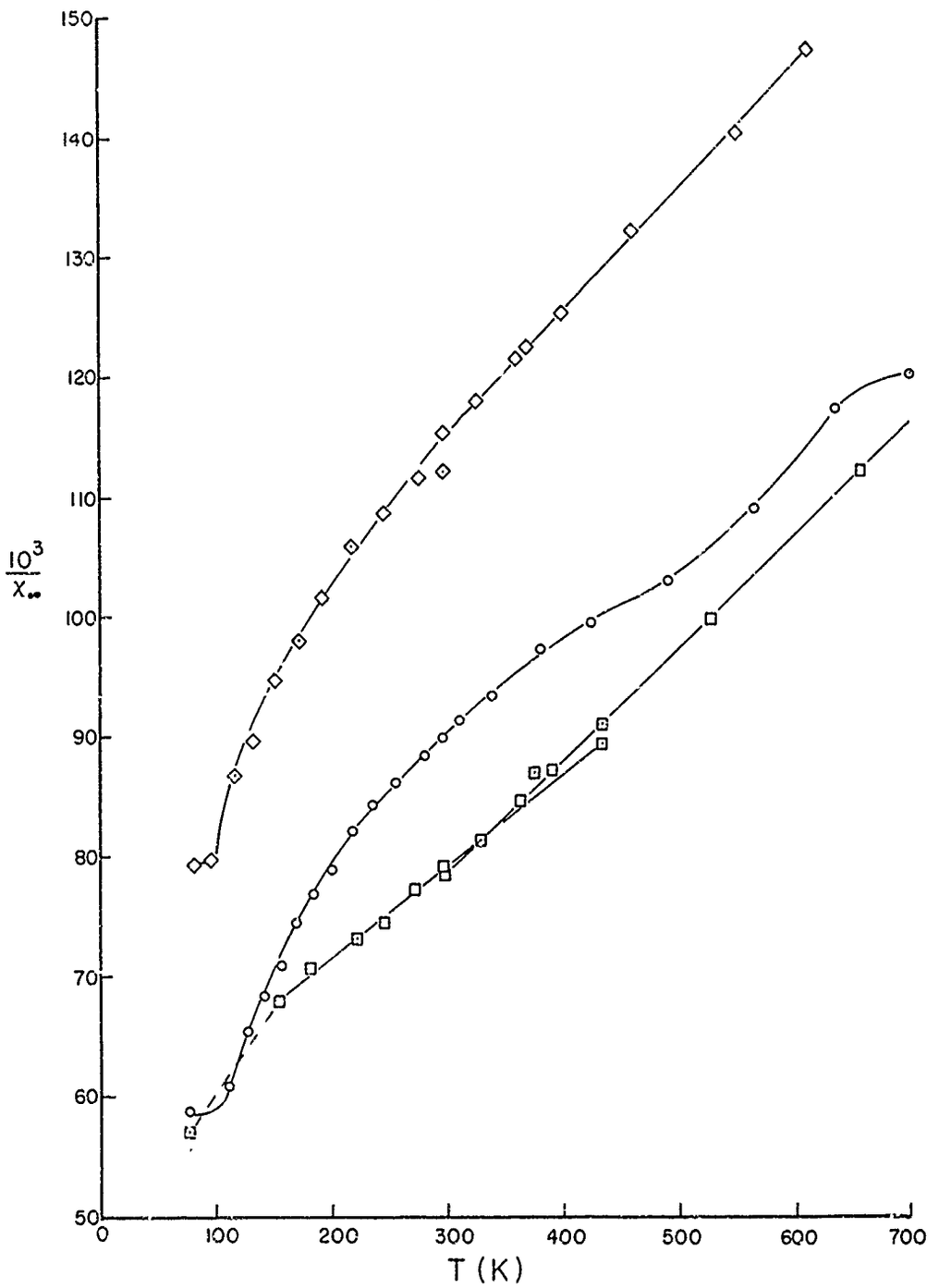

FIGURE 4. Inverse high-field susceptibility of hexagonal $LuMn_{1-x}Fe_xO_3$ solid solutions. χ_∞ in units of μemu/gm. Diamonds: $LuMn_{.75}Fe_{.25}O_3$; circles: $LuMn_{.5}Fe_{.5}O_3$; squares: $LuMnO_3$.

not really a well-defined quantity and it is not surprising that the high-temperature points (obtained by the same extrapolation method as the lower-temperature ones) do not fall on quite the same line. In contrast, the susceptibilities of the solid solutions show no field dependence, but a strong temperature dependence; so that the conventional analysis in terms of effective moments and paramagnetic Curie temperatures has little meaning. For both solid solutions, the susceptibility curves appear to flatten out below 100 to 110 K. This probably indicates an antiferromagnetic transition at this point; additional data are being taken to confirm this. It is not known why the transition should be apparent in the solid-solution susceptibility when it is not so in $LuMnO_3$, nor why $LuMn_{.75}Fe_{.25}O_3$ has a much lower susceptibility than the other materials.

iii) $YbCr_{1-x}Mn_xO_3$ - Susceptibility work on this system was continued with remeasurements on hexagonal $YbCr_{.05}Mn_{.95}O_3$ and orthorhombic $YbCrO_3$ and $YbCr_{.75}Mn_{.25}O_3$ and with new measurements on the high-pressure-transformed orthorhombic forms (for which there is complete solid solution) with compositions $YbCr_{.5}Mn_{.5}O_3$, $YbCr_{.25}Mn_{.75}O_3$, and $YbCr_{.1}Mn_{.9}O_3$. All these measurements were from helium temperature to above room temperature. The remeasurements with the modified apparatus confirmed the general features discussed in the Annual Report low temperature moments in all three materials, and a compensation point at about 18 K in $YbCrO_3$ (Fig. 5). The moment below 50 K in $YbCr_{.05}Mn_{.95}O_3$ is much too large to be attributable to a second phase of $YbCr_{.75}Mn_{.25}O_3$ in the sample. This is the only hexagonal material found so far which has an intrinsic ferromagnetic moment. Since it lies at the composition limit, it is not clear how the Curie temperature could be increased easily. There are small differences in magnetic

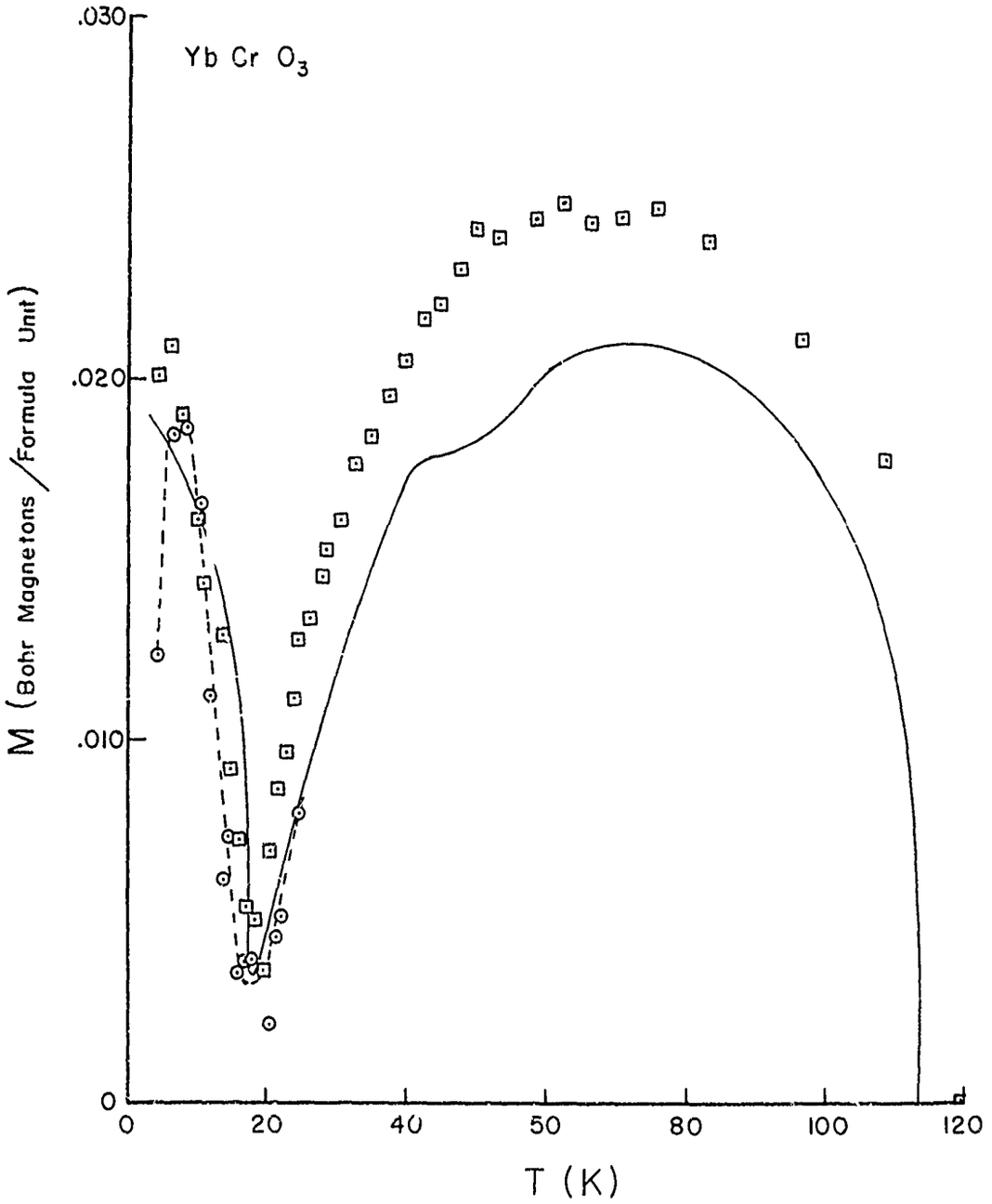

FIGURE 5. Spontaneous magnetic moment in $YbCrO_3$. Solid curve is taken from Annual Report. Circles and squares are results from two new runs with modified apparatus (see text). Data from one run was not analyzed above 25 K because of rapid susceptibility changes due to adsorbed oxygen. The slight dip at 40-50 K in the solid curve is probably also a data-analysis artifact resulting from a small amount of adsorbed oxygen. The vertical scale is not highly accurate because of the small mass of the samples.

properties between the two samples (from the same lot). These differences need to be investigated further; there remains a slight possibility that the moment is due to some sort of Mn-Cr spinel impurity. The low temperature properties of the orthorhombic samples have not yet been analyzed in detail, but the Curie temperature appears to decrease rapidly with increasing Mn content. The high temperature properties of all the samples are summarized in Figure 6. There appears to be a possibility that orthorhombic $YbCr_{1/3}Mn_{2/3}O_3$ might be metamagnetic or ferrimagnetic.

NARROW-BAND NARROW-GAP MATERIALS

Background

Many potential applications for solid state integrated circuits cannot be realized because high-speed switching elements have not yet been developed. This circumstance has stimulated a great deal of interest in materials which undergo abrupt semiconductor (or insulator)-to-metal transitions. Of greatest practical importance are materials in which such transitions can be induced by an applied electric field. In addition, it is highly desirable that the switching mechanism be purely electronic without the necessity for secondary (usually slower) mechanisms such as thermal effects which play an important role in the chalcogenide glasses. To date, an electric-field-induced electronic transition appears to have been observed only in V_2O_3 and VO_2. In the latter case, at least, it is said that the transition results from huge piezoelectric strain[19] but this seems to contradict the observed crystal symmetry.[20] One might expect purely electronic transitions in materials which possess loosely-bound localized excited states, and indeed such states have been invoked to explain the

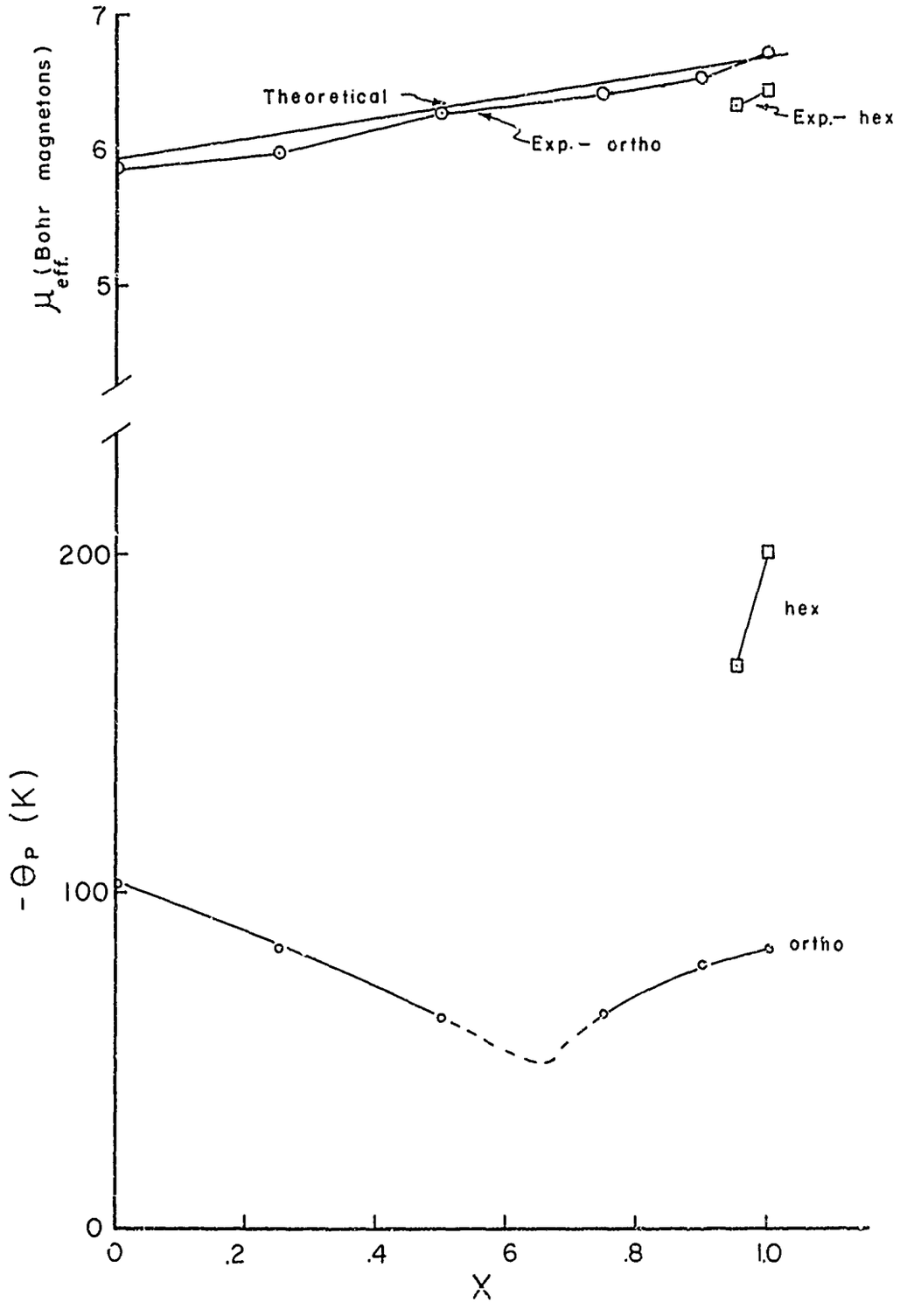

FIGURE 6. High-temperature magnetic parameters of $YbCr_{1-x}Mn_xO_3$ solid solutions.

electrical behavior of certain compounds containing divalent samarium ions. In particular, the gradual semiconductor-to-metal transition as a function of temperature in SmB_6 has been interpreted in this way. Nickerson, et al.[21] suggested that this behavior might be unique to SmB_6 owing to the extreme rigidity of the boron lattice. However, a rather similar, although pressure-induced, transition has been discovered by Jayaraman[22] in SmS. But this transition seems rather peculiar, since the resistivity and magnetic susceptibility[23] show large hysteresis effects which are not apparent in the lattice parameter changes even though the volume change at the transition is very large. Conductivity transitions have also been observed in SmSe and SmTe, both of which have a much higher off-state resistivity than SmS, but in these cases the pressure-induced transitions are not abrupt.[24] In order to understand better the mechanisms for conductivity transitions in these samarium monochalcogenides we have recently been studying some $SmS_{1-x}Se_x$ solid solutions. Some of these should have abrupt transitions, like SmS, but with an off-state – on-state resistivity ratio which is more typical of that desired for a switch.

In what follows, we describe first the preparation and characterization of chalcogenide samples, as well as of Sm_4As_3, the only other compound worked on during the present report period. Following this, we discuss the temperature and pressure variation of the resistivity in the only sample in which these have been studied so far, of nominal composition $SmS_{.75}Se_{.25}$. Finally, the interesting strong white cathodoluminescence seen on some samples is described.

Preparation and Characterization

Preparation and Crystal Growth of SmS_xSe_{1-x}

The samarium monochalcogenides have previously been prepared[25] by reacting samarium metal filings or turnings with the Group VI elements at moderate temperatures (e.g., 400-850 C) in sealed silica ampoules. Subsequently the material was melted in a tantalum crucible in an inert atmosphere to form a polycrystalline fused ingot that usually contained large crystals from which single-crystal specimens of accpetable size could be cleaved or cut. Work on the preparation of SmS-SmSe solid-solution material was initiated using these general procedures (See Annual Report). The low-temperature synthesis, in which reaction temperatures of 400 - 600 C were used, appeared to be satisfactory. However, melting the materials (by use of an rf field) and refreezing in an open tantalum crucible yielded apparent single-phase crystals only in one case, for a composition $SmS_{.75}Se_{.25}$. As indicated in Table 4, initial specimens of $SmS_{.5}Se_{.5}$ and $SmS_{.9}Se_{.1}$ had a second phase, $Sm_3(S,Se)_4$, of Th_3P_4 structure, indicating preferential loss of samarium. Specimens prepared in the period covered by this report were prepared by melting in evacuated, sealed tantalum crucibles that were sealed by electron-beam welding. The specimens were melted (maximum temperature 2050 C) and, with the specimen in a temperature gradient of $\sim$ 25 C/cm, were cooled at a rate of $\sim$ 25 C/hour, thus directionally freezing the material. The initial pair of specimens so prepared, -44 and -45 in Table 4, were made slightly samarium-rich to compensate for anticipated loss of samarium to the vapor space. These specimens were found to be polyphase, with minor amounts of samarium-rich material present as an eutectic phase.

TABLE 4. SUMMARY ON PREPARATION OF BULK SPECIMENS OF SmS_xSe_{1-x}

Specimen No.	Initial Composition	Preparation Conditions	Results
28886-26	$SmS_{.5}Se_{.5}$	Melted and directionally crystallized in unsealed Ta crucible.	Sm(S,Se) plus $Sm_3(S,Se)_4$ second phase
28886-28	$SmS_{.9}Se_{.1}$	"	"
28147-89	$SmS_{.75}Se_{.25}$	"	$SmS_{.75}Se_{.25}$
28886-44	$Sm_{1.01}S_{.6}Se_{.4}$	Melted and directionally crystallized in evacuated, sealed Ta crucible	Sm(S,Se) plus Sm-rich phase of approx. composition $Sm_4(S,Se)_3$.
28886-45	$Sm_{1.01}S_{.8}Se_{.2}$	"	"
28886-57	$SmS_{.6}Se_{.4}$	"	Fused material: fcc $SmS_{.6}Se_{.4}$ phase. Vapor deposit above melt: fcc $SmS_{.6}Se_{.4}$ phase with very fine Widmanstatten-like precipitates.
28886-58	$SmS_{.8}Se_{.2}$	"	Fused material: fcc $SmS_{.8}Se_{.2}$ phase plus minor $Sm_3(S,Se)_4$ phase. Vapor deposit above melt: fcc $SmS_{.8}Se_{.2}$ crystals with chalcogenide-deficient, Widmanstatten-like precipitate.

Phase analyses refer only to phases observed by optical metallography with composition determined by electron-probe microanalysis.

Electron microprobe analysis indicated that the composition of this eutectic phase corresponded to $Sm_4(S,Se)_3$. The amount of this second phase was too small for extraction and separate crystal structure analysis.

When stoichiometric charges (specimens -57 and -58) were melted in the sealed containers, crystals grown from the vapor phase were found adhering to the tantalum above the main fused samples in the bottom of the container. The specimen -57 of $SmS_{.8}Se_{.2}$ had disproportionated, with the fused material being samarium deficient and the vapor-phase deposit having excess samarium. The fused material, in addition to face-centered cubic $SmS_{.8}Se_{.2}$ with a_o = 6.018Å, had minor phases of $Sm_3(S,Se)_4$ with the Th_3P_4 structure. The vapor-deposited material had the face-centered cubic phase, $SmS_{.8}Se_{.2}$ (a_c = 6.018Å). Metallographic examination showed Widmanstatten-like short acicular precipitates. Electron-probe microanalysis showed that these precipitates were deficient in S, corresponding to $Sm_4(S,Se)_3$. The main fused material in specimen -58 of $SmS_{.6}Se_{.4}$ appeared to be single-phase and face-centered cubic with a_o = 6.048Å. The vapor-deposited material had very fine acicular precipitates, similar to those described above for $SmS_{.8}Se_{.2}$. The main phase was face-centered cubic $SmS_{.6}Se_{.4}$, the same as for the fused material. Thus it appears that, owing to the disproportionation, preparation of large stoichiometric crystals may be difficult. The samples with minor dispersed precipitates should be satisfactory for most purposes, however, and measurements are being made on some of them. It should be noted that in one case (see below), a minor interfacial phase not apparent by optical metallography was put into evidence by the electron microprobe.

Preparation and Crystal Growth of Sm_4As_3

Work on the preparation of specimens of Sm_4As_3 has followed the general procedures just described for the preparation of the chalcogenides. The compound first is prepared by the low-temperature (400-600 C) reaction of the elements in silica containers. The material then is melted and recrystallized in evacuated, sealed tantalum crucibles. However, in the case of the arsenides, overall sample composition has been selected in the samarium-rich range (Sm_2As to $Sm_{1.5}As$) to give crystallization at moderate temperatures (1500-1750 C) from solution in excess samarium. Directional freezing has been produced by dropping the crucible from the high-temperature zone at a rate of 1 mm/hour.

Results obtained to date indicate that Sm_4As_3 is a peritectic phase that must be obtained by solid-state reaction or by crystallization from solution (e.g., in excess samarium). A charge of overall composition Sm_2As failed to melt at 1500 C, but was entirely melted at 1750 C. When slowly cooled from 1750 C and directionally frozen, the charge appeared to consist of about equal parts of SmAs (first to freeze) and Sm_4As_3 (last to freeze). The SmAs crystals were of about 0.5 cm dimensions and appeared to be of good quality; their electrical properties will be investigated in view of the recent reopening by Wachter[26] of the question of semiconductivity. The results suggest that single-phase Sm_4As_3 can be crystallized from initial melt compositions containing somewhat higher concentrations of samarium.

Resistivity Measurements

As discussed above, single-phase specimens of $SmS_{1-x}Se_x$ compounds are quite difficult to prepare. Furthermore, X-ray diffraction techniques do not provide an entirely adequate test of sample homogeneity. This is the technique that has been most widely used to characterize specimens which exhibit conductivity transitions, but it should be regarded as only a preliminary screening test for electrical property measurements. As is apparent from Table 4, prior to our most recent preparations only one $SmS_{1-x}Se_x$ specimen showed sufficient homogeneity to warrant electrical property characterization, and this sample of $SmS_{.75}Se_{.25}$, is the only one so far studied this way. The electrical resistivity and Hall coefficient of this specimen were measured over the temperature range 100-400 K. As seen in Fig. 7, the electrical resistivity shows two regions of typical semiconducting behavior with a small change in activation energy occurring near 200 K. At room temperature the pertinent electrical data for this specimen are: resistivity, 1.205 Ω cm; mobility, 11 cm^2/volt sec; carrier concentration, 4.8×10^{17} cm^{-3} and Hall coefficient, - 13 cm^3/coul. In comparison, Fig. 8 is a reproduction of the resistivity data obtained by Darnell et al. (Atomics International Report to ARPA, June 1971) for ceramic samples of various compositions in the $SmS_{1-x}Se$ system. A few points are worth noting. For the specimen having the same composition as reported here, Darnell et al. found a smaller activation energy in the range 300 to 400 K and a much lower room temperature resistivity (about 0.085 Ω cm). These results indicate, at least superficially, that our specimen is of better electrical quality. It is probably fortuitous that the overall temperature dependence of the electrical resistivity of our $SmS_{.75}Se_{.25}$

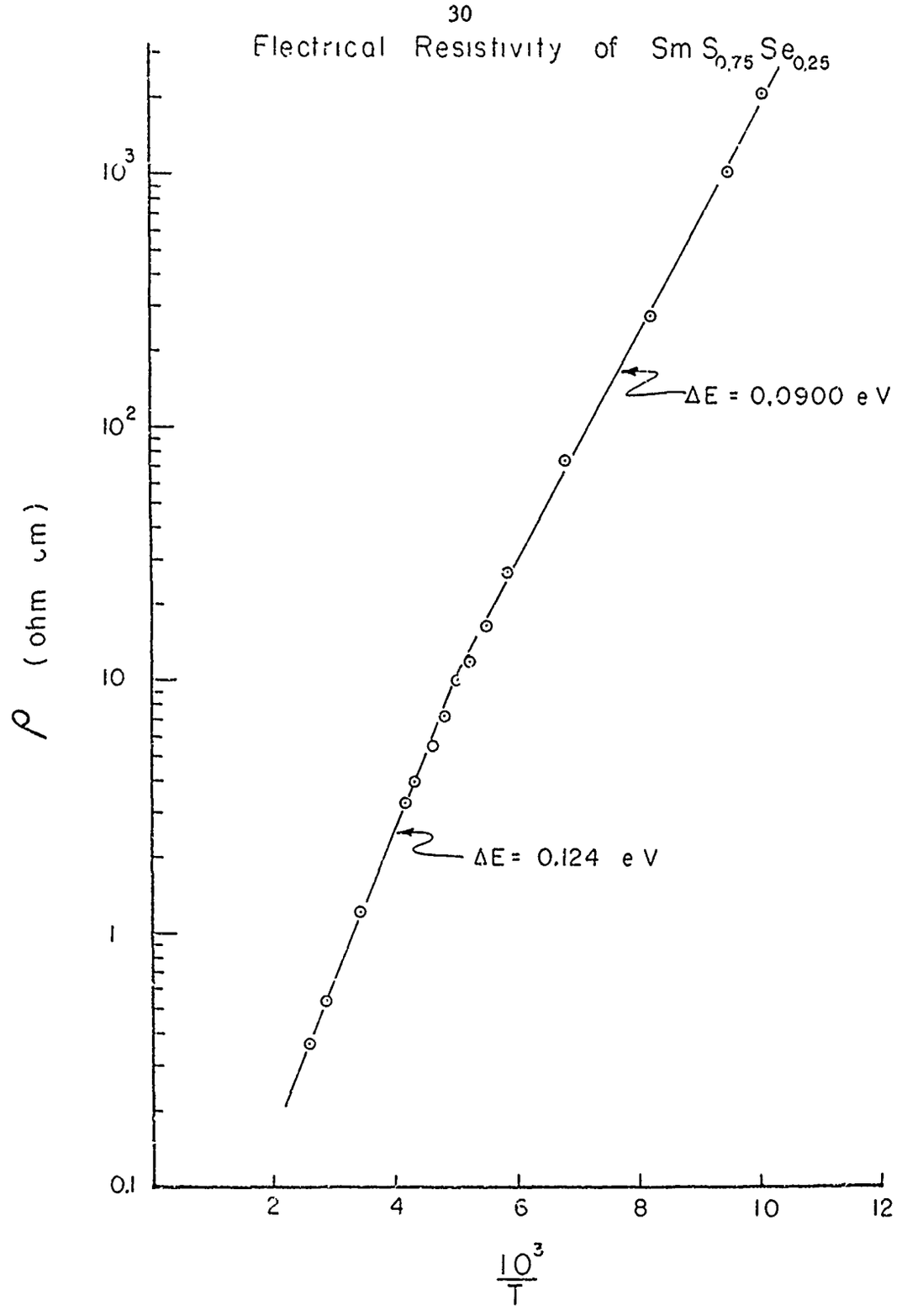

FIGURE 7. Electrical resistivity of polycrystalline sample of $SmS_{.75}Se_{.25}$.

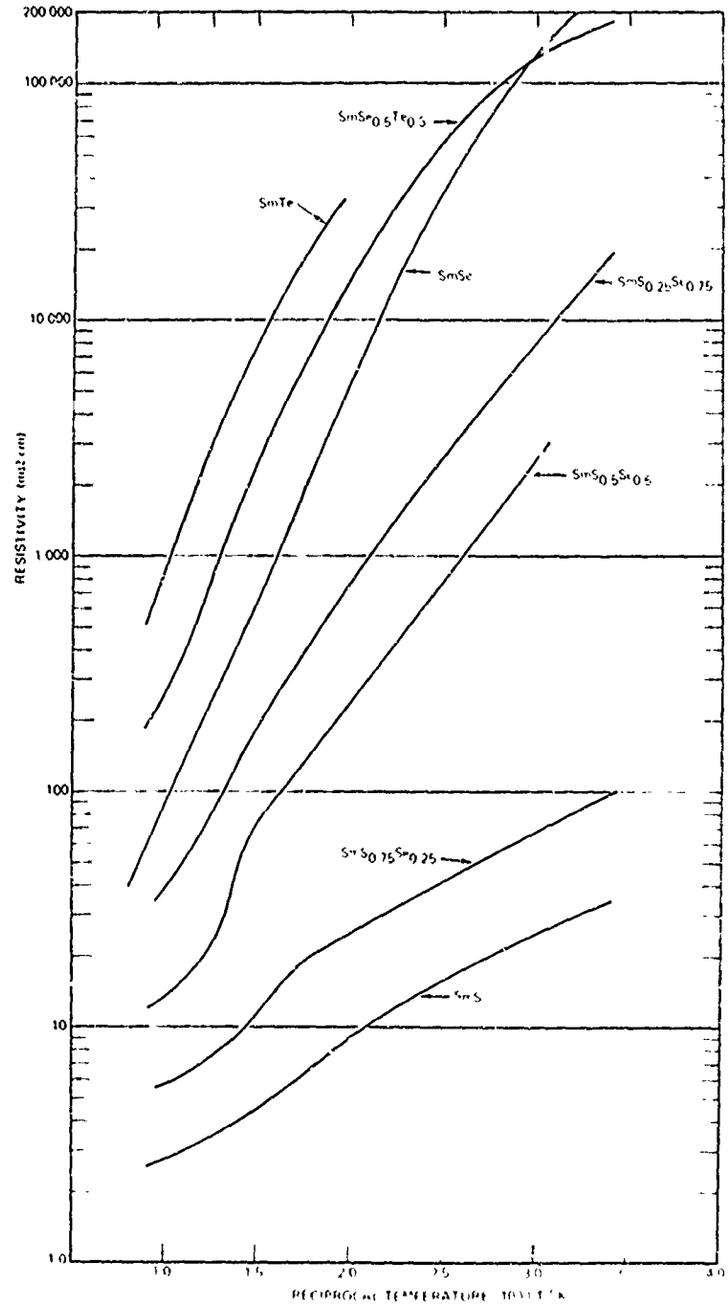

FIGURE 8. Electrical resistivities of ceramic samples of samarium chalcogenide solid solutions
(after Darnell et al, Report AI-71-28 (June 1971), see text, p. 29).

specimen is similar to that found by Darnell et al. for their $SmS_{.50}Se_{.50}$ specimen. The principal point is that the room temperature resistivity of our $SmS_{.75}Se_{.25}$ specimen is almost an order of magnitude higher than that shown in Fig. 8, and reported elsewhere,[22] for SmS. Thus in terms of an electronic switch, a specimen of this composition would appear to have greater potential than SmS because the "off state" resistivity should be much higher. Encouraged by these results, we performed resistivity measurements as a function of pressure and made microstructure analyses on the $SmS_{.75}Se_{.25}$ specimen. The pressure dependence of the resistivity is shown in Fig. 9. Unlike the SmS samples of Jayaraman et al.,[22] our sample did not crack when the pressure was reduced. There is seen to be a discontinuous transition at 18 kbar with a resistance drop of about two orders of magnitude (curve 1); the resistivity does <u>not</u> however return to the original value, but to a considerably lower value (curve 2). Upon recycling the pressure, a gradual transition to the high conductivity state takes place (curve 3) similar to that occurring at higher pressure in SmSe, and on releasing the pressure the resistivity returns to its value at the start of the second cycle (curve 4). The apparently irreversible transformation led us to examine the microstructure of the sample more closely. We found by electron microscopy (Fig. 10a) that the original material contained a continuous grain boundary phase, not apparent from optical metallography, of approximate composition $Sm_4(S,Se)_3$. After the pressure cycles, this continuous phase had disappeared, a sulfur-rich droplet-like precipitate phase of composition near $SmS_{.90}Se_{.1}$ appearing instead (Fig. 10b). If we assume that the boundary $Sm_4(S,Se)_3$ phase is of high resistivity, then it appears likely that the discontinuous transition is due to the

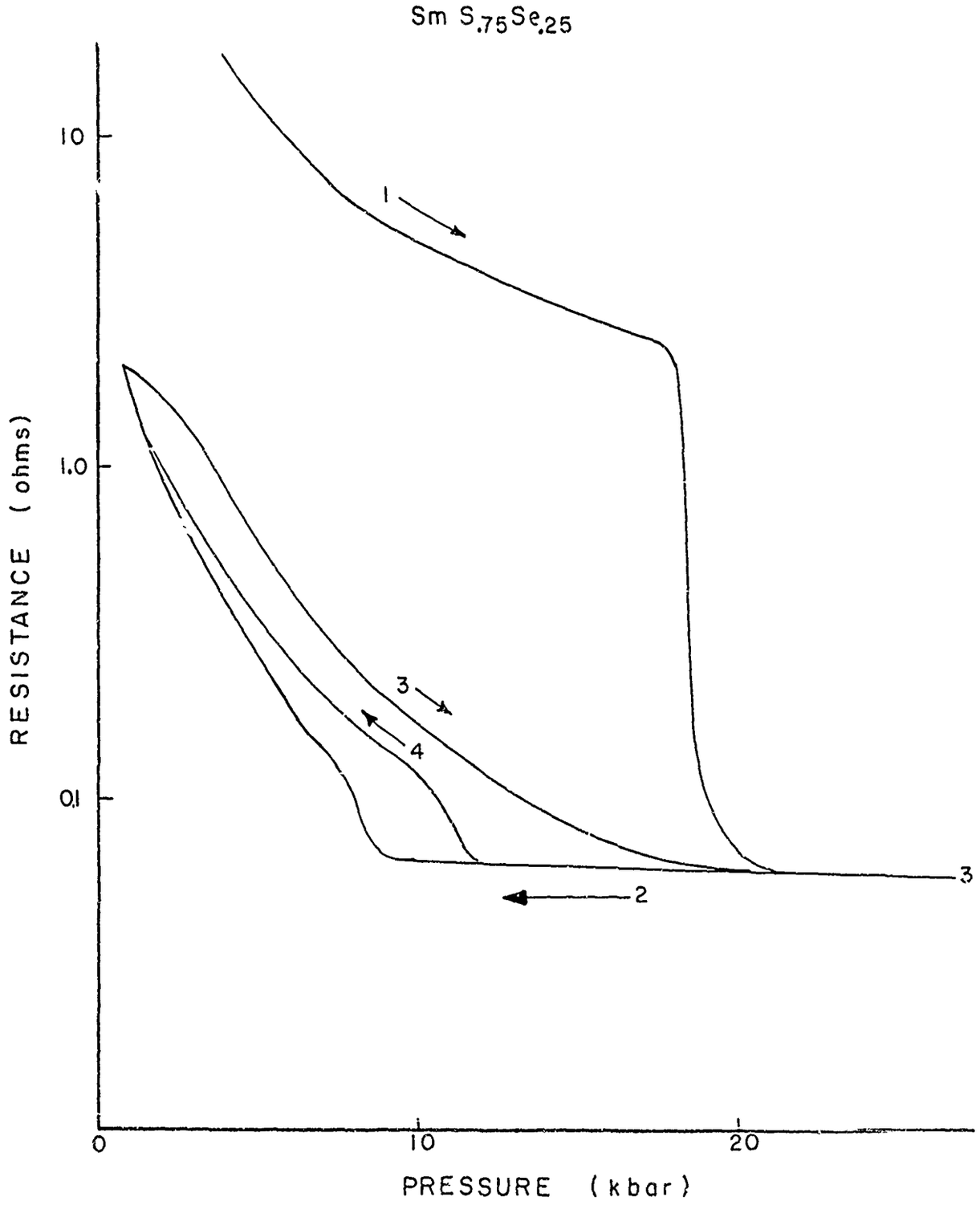

FIGURE 9. Pressure variation of resistance of polycrystalline sample of $SmS_{.75}Se_{.25}$. See text (p. 32) for detailed discussion of cycles.

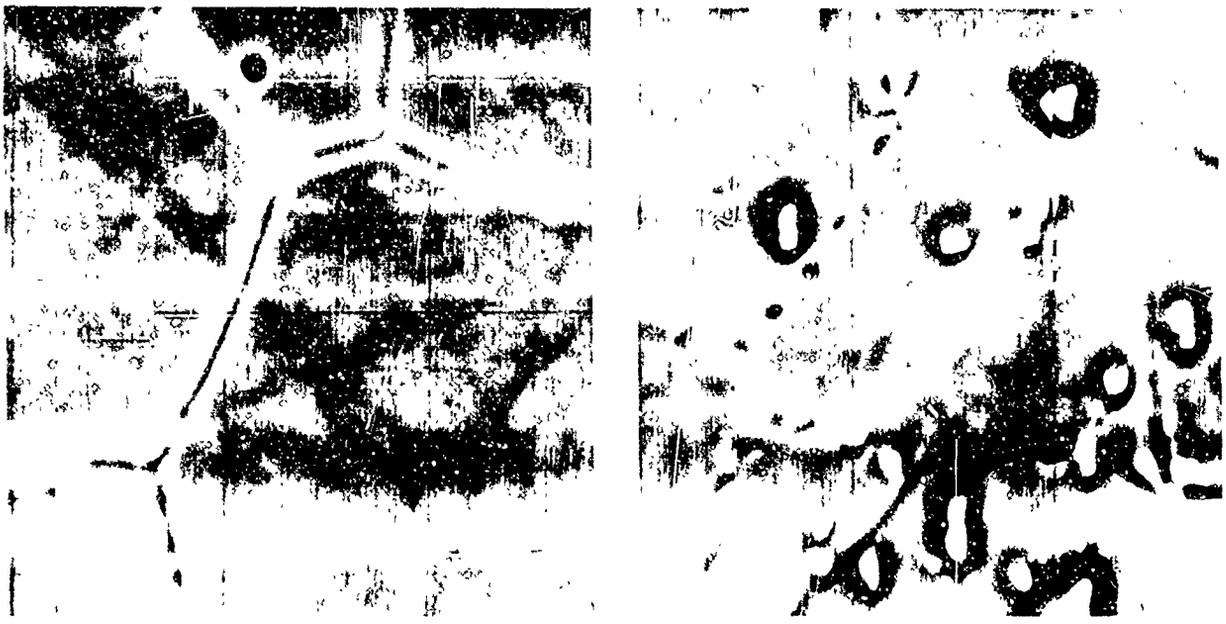

(a) Before pressure cycle (b) After pressure cycle

FIGURE 10

Electron Beam Images of $SmS_{.75}Se_{.25}$ Specimen 28147-89

The left micrograph shows the continuous grain-boundary phase as a dark line with a gradient white band into the adjacent grain. The right micrograph shows the breakup of this grain-boundary phase after application of high pressure, 18 kbar. Here the grain boundaries have discrete precipitates. (The separate white spots within black ones are pits in the surface.) Magnification approximately 1200X.

breaking-up of this phase under pressure, and that the second cycle is more characteristic of $SmS_{.75}Se_{.25}$. Since detailed microstructure analyses have not been reported on samples studied elsewhere, the possibility immediately suggested itself that the same effect might be responsible for the discontinuous transition in pure SmS.

In order to test this point and to define more clearly the role of minor phases in the conductivity transition, we are undertaking similar studies on SmS, $SmS_{.80}Se_{.20}$ and $SmS_{.60}Se_{.40}$. Measurements of resistivity as a function of temperature on the transformed sample are also being done in order to show the extent to which the initial measurements were representative of the majority phase. It should be noted, though, that very recent magnetic susceptibility measurements[27] on SmS appear to indicate a discontinuous transition with hysteresis through two cycles. Moreover, some of the resistivity measurements[22] on SmS are believed to have been on single crystals.

Cathodoluminescence

Strong cathodoluminescence was observed from samples of $SmS_{.6}Se_{.4}$ and $SmS_{.8}Se_{.2}$ in the course of electron microprobe analysis. Both the bulk fused and vapor-deposited material of $SmS_{.6}Se_{.4}$ exhibited the luminescence, but only the vapor-deposited $SmS_{.8}Se_{.2}$ did so. The luminescence appeared white and, above about 0.2 watt power, was much brighter than the incident illumination on the specimen surface. The spectral distribution was a broad maximum at about 540 mμ as shown in Fig. 11. The spectra from the $SmS_{.6}Se_{.4}$ samples were measured for incident electron beams of 25 to 45 kv with currents from 1 to . μamp, or power from 0.07 to 0.6 watts. The intensity increases with t' . electron beam current and power without appreciable shift in distribution. The power density is

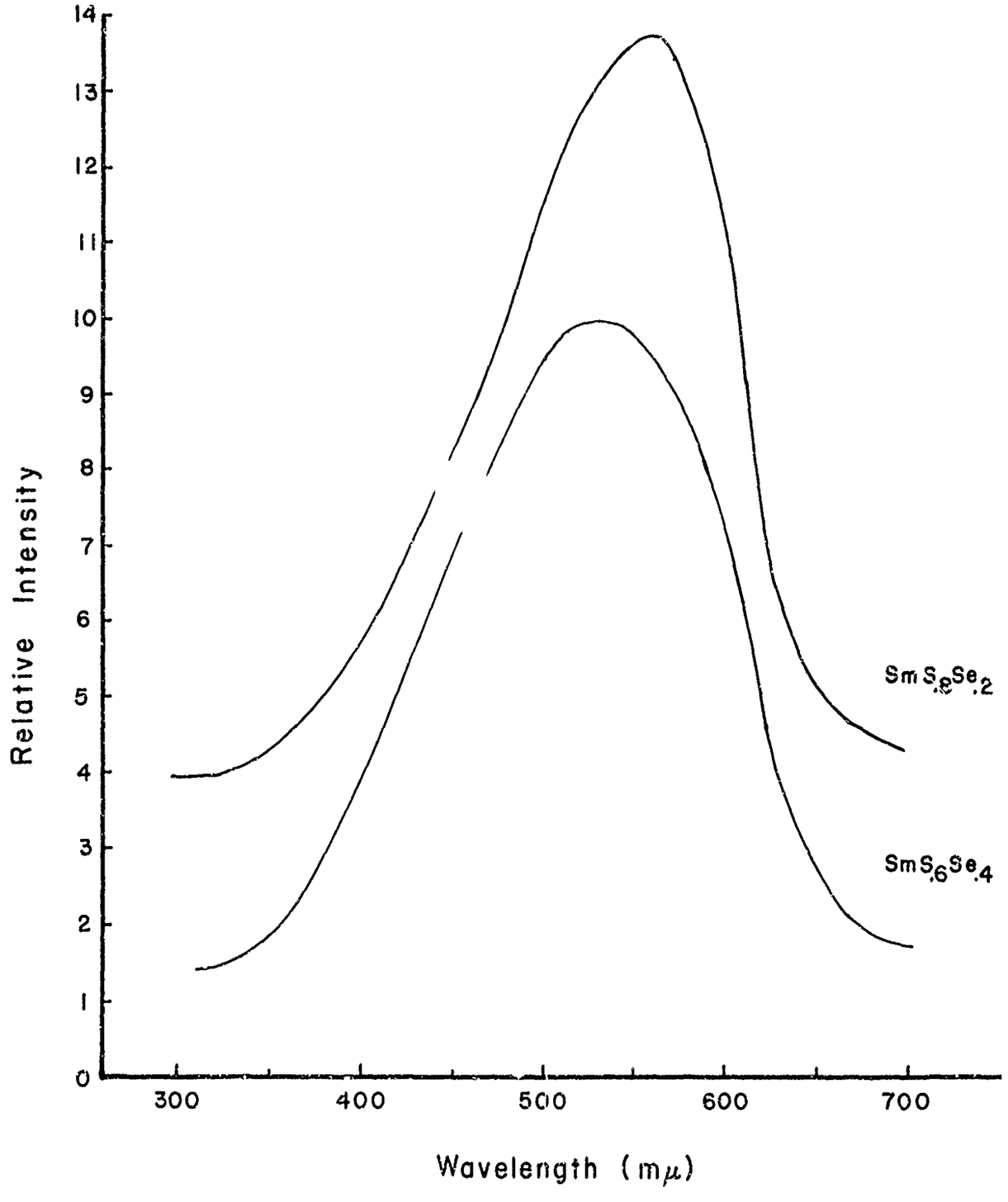

FIGURE 11. Cathodoluminescence, at reduced power, of polycrystalline samples of $SmS_{.8}Se_{.2}$ and $SmS_{.6}Se_{.4}$. (Both curves shifted upwards from zero intensity at ends.) Beam voltage 45 kV, current 2 μamp. Spectrometer resolution 15 mμ or better.

very high, of course, since the electron beam impinges on an area of order 1 square micron. This luminescence appears sufficiently strong to bear comparison with Gd_2O_2S and other commercial white phosphors.

REFERENCES

1. T. F. O'Dell, Electrodynamics of Magnetoelectric Media (North Holland, 1970): S. M. Skinner, IEEE Trans. PMP-6, 68 (1970); L. N. Bulaevskii and V. M. Fain, JETP Letters 8, 165 (1968); A. I. Akhiezer and I. A. Akhiezer, Sov. Phys. JETP 32, 552 (1971); I. A. Akhiezer and L. N. Davydov; Sov. Phys.-Solid State 12, 2563 (1971); V. G. Baryakhtar and I. E. Chupis, Sov. Phys.-Solid State 10, 2818 (1969); V. N. Lyubimov Sov. Phys.-Crystallog. 13, 877 (1969); E. Ascher, J. Phys. Soc. Japan 28, (Suppl.) 7 (1970), among more recent references.

2. W. F. Brown, Jr. et al., Phys. Rev. 168, 574 (1968).

3. E. F. Bertaut et al., Comptes Rendus 256, 1958 (1963); R. Pauthenet and C. Veyret, J. de Physique 31, 65 (1970).

4. C. N. R. Rao and G. V. Subba Rao, Proc. 8th Rare Earth Research Conf. (Reno 1970), 653; G. V. Subba Rao et al., J. Phys. Chem. Solids 32, 345 (1971).

5. P. Coeure, Solid State Communs. 6, 129 (1968); see also J. P. van der Ziel and L. G. van Uitert, Phys. Rev. 179, 343 (1969).

6. A. S. Viskov et al., Inorganic Materials 4, 71 (1968).

7. E. Ascher et al., J. Appl. Phys. 37, 1404 (1966); H. Schmid et al., Solid State Comm. 3, 327 (1965).

8. I. G. Ismailzade and S. A. Kizhaev, Sov. Phys.-Solid State 7, 236 (1965).

9. M. Marezio et al., Acta Cryst. B26, 2008 (1970).

10. H. Tamura et al., Japan J. Appl. Phys. 4, 621 (1965).

11. R. Linares, J. Am. Ceram. Soc. 45, 307 (1962).

12. T. Telmlee and R. Hiskes, Final Tech. Rept., Contract DAAH01-70-C-1106 (June 1971) (AD 885334L).

13. R. Barks and D. Roy, p 497 in Crystal Growth, (H. Peiser, ed.), (Pergamon Press, London, 1967).

14. J. Remeika, J. Am. Chem. Soc. 78, 4259 (1956).

15. W. Kunnmann et al., J. Phys. Chem. Solids 26, 311 (1965).

16. H. Koizumi et al., Japan J. Appl. Phys. 3, 495 (1964); E. Speranskaya et al; Bull. Acad. Sci. USSR, Div. Chem. Sci., #5, 873 (1965).

17. A. Apostolov and P. Pataud, Mat. Res. Bull. 4, 1 (1969).

18. V. P. Polyakov et al., Sov. Phys.-Solid State 11, 1147 (1969).

19. K. A. Valiev et al., JETP Letters 12, 12 (1970); Sov. Phys.-Solid State 13, 342 (1971).

20. G. Andersson, Acta Chem. Scand. 10, 623 (1956).

21. J. C. Nickerson et al., Phys. Rev. B3, 2030 (1971).

22. A. Jayaraman et al., Phys. Rev. Letters 25, 1430 (1970).

23. M. B. Maple and D. Wohlleben, Phys. Rev. Letters 27, 511 (1971).

24. A. Jayaraman et al., Phys. Rev. Letters 25, 368 (1970).

25. J. F. Miller, et al., Air Force Avionics Lab. Rept. ALTDR 64-239, Contract AF 33(657)-10687 (Battelle), (1964).

26. D. Wohlleben et al., Proc. 17th Conf. on Magnetism and Magnetic Materials, Chicago 1971 (to appear).